A New Mechanism for Nucleation beneath Monolayer Films?

S. J. Cooper,*,† R. B. Sessions,‡ and S. D. Lubetkin§

Contribution from the H. H. Wills Physics Laboratory, University of Bristol, Tyndall Avenue, Bristol, BS8 1TL, UK, Department of Biochemistry, University of Bristol, University Walk, Bristol, BS8 1TD, UK, and DowElanco, 9330 Zionsville Road, Indianapolis, Indiana 46268

Received October 31, 1996. Revised Manuscript Received December 10, 1997

Abstract: The nucleation of the amino acids, aspartic acid and asparagine monohydrate, beneath monolayer films has been investigated as a function of film material and surface pressure. For the first time, nucleation has been shown to occur preferentially beneath films at low to medium surface pressures and not at high surface pressures as previously found. At high surface pressures, where the film was close-packed, the nucleation rate was low. In contrast, the nucleation rate was optimum under films at low to medium surface pressures. Since the close-packed films were unable to induce significant nucleation promotion, it is highly unlikely that this optimum nucleation at lower surface pressures occurs beneath close-packed film islands, but rather it is induced by the inherent nature of the films at lower surface pressures. We believe these novel results arise from both the substantial adsorption of the amino acid zwitterions between the film molecules and the exploitation of the greater compressional freedom of films at lower surface pressures, which enables greater lattice mismatches between the film and nucleating crystal face to be accommodated. Based on these findings, a new mechanism for nucleation beneath monolayer films is proposed. By using molecular modeling it was possible to demonstrate the existence of an electrostatic and geometric correlation between the film and nucleating crystal face in all cases. Therefore nucleation beneath the monolayers was governed by both strong adsorption upon the film and a correspondence between the structure and geometry of the film and nucleating crystal face, the latter correspondence being facilitated by the greater compressibility of the lower surface pressure films.

Introduction

It is known that monolayer films can act as sites upon which heterogeneous, and indeed epitaxial, nucleation may preferentially occur.[1,2] The resulting nucleation is often highly specific; either a particular crystal morphology[1−6] or polymorph[7−11] may be obtained by careful choice of the film material. Hence, this phenomenon has important implications in the fields of both crystal morphological engineering[12] and biomineralization.[7,10]

Nucleation beneath monolayer films relies upon a degree of molecular recognition between the film and nucleating species. This recognition may be manifested by an exact match of the film headgroup to the nucleating species, usually called "template matching", whereby the film mimics a particular plane in the nucleating crystal and so leads to nucleation bounded by this plane.[1−6] Alternatively, electrostatic attraction and either geometrical matching, or stereochemical complementarity, may be sufficient to bias the nucleation to the required outcome;[7−11] this is observed in biomineralization.[10]

Original monolayer crystallization experiments[1,2] concentrated upon producing nucleation under films compressed to high surface pressures, where the film was known to be in a close-packed and essentially fully ordered state. Thus, these films acted as 2D crystals, producing a corresponding order in any material that adsorbed strongly upon them. Oriented nucleation has since been obtained,[3−5,7,8,13,14] however, on partially compressed or uncompressed films, albeit at a reduced rate. Lahav et al. suggested[3] that such epitaxial nucleation occurred on condensed, close-packed film islands that coexisted with the more expanded film, and, for some of the monolayers used, these islands were shown to exist.[4,5,14−17] In monolayers with aliphatic chains, close-packed film island formation is not generally observed at room temperature and low surface pressures.[16,18−20] Indeed, close-packed film island formation is only observed if the aliphatic chain is fluorinated,[15] or the

* To whom correspondence should be addressed.
† H. H. Wills Physics Laboratory, University of Bristol.
‡ Department of Biochemistry, University of Bristol.
§ DowElanco.

(1) Landau, E. M.; Levanon, M.; Leiserowitz, L.; Lahav, M.; Sagiv, J. *Nature* **1985** *318*, 353−356.
(2) Landau, E. M.; Popovitz-Biro, R.; Levanon, M.; Leiserowitz, L.; Lahav, M.; Sagiv, J. *Mol. Cryst. Liq. Cryst.* **1986**, *134*, 323−335.
(3) Landau, E. M.; Grayer Wolf, S.; Levanon, M.; Leiserowitz, L.; Lahav, M.; Sagiv, J. *J. Am. Chem. Soc.* **1989**, *111*, 1436−1445.
(4) Weissbuch, I.; Berkovic, G.; Yam, R.; Als-Nielson, J.; Kjaer, K.; Lahav, M.; Leiserowitz, L. *J. Phys. Chem.* **1995**, *99*, 6036−6045.
(5) Popovitz-Biro, R.; Wang, J. L.; Majewski, J.; Shavit, E.; Leiserowitz, L.; Lahav, M. *J. Am. Chem. Soc.* **1994**, *116*, 1179−1191.
(6) Tang, R.; Tai, Z.; Chao, Y. *Chem. Lett.* **1996**, *7*, 535−536.
(7) Mann, S.; Heywood, B. R.; Rajam, S.; Birchall, J. D. *Nature* **1988**, *334*, 692−695.
(8) Mann, S.; Heywood, B. R.; Rajam, S.; Birchall, J. D. *Proc. R. Soc. London* **1989**, *A423*, 457−471.
(9) Mann, S.; Heywood, B. R.; Rajam, S.; Walker, J. B. A.; Davey, R. J.; Birchall, J. D. *Adv. Mater.* **1990**, *2*, 257−261.
(10) Heywood, B. R.; Mann, S. *Adv. Mater.* **1994**, *6*, 9−20.
(11) Heywood, B. R.; Mann, S. *Chem. Mater.* **1994,** *6*, 311−318.
(12) Weissbuch, I.; Popovitz-Biro, R.; Lahav, M.; Leiserowitz, L. *Acta Crystallogr.* **1995**, *B51*, 115−148.
(13) Weissbuch, I.; Frolow, F.; Addadi, L.; Lahav, M.; Leiserowitz, L. *J. Am. Chem. Soc.* **1990**, *112*, 7718−7724.
(14) Weissbuch, I.; Berkovic, G.; Leiserowitz, L.; Lahav, M. *J. Am. Chem. Soc.* **1990**, *112*, 5874−5875.
(15) Jacquemain, D.; Grayer Wolf, S.; Leveiller, F.; Lahav, M.; Leiserowitz, L.; Deutsch, M.; Kjaer, K.; Als-Nielson, J. *J. Am. Chem. Soc.* **1990**, *112*, 7724−7736.
(16) Jacquemain, D.; Leveiller, F.; Weinbach, S. P.; Lahav, M.; Leiserowitz, L.; Kjaer, K.; Als-Nielson, J. *J. Am. Chem. Soc.* **1991**, *113*, 7684−7691.

S0002-7863(96)03799-7 CCC: $15.00
Published on Web 02/18/1998

temperature is reduced close to freezing.[16,17] Mann *et al.*,[7,8] working on the preferential nucleation of the less stable polymorph, vaterite, of calcium carbonate beneath octadecanoic acid monolayers, showed that while the fully compressed films produced a greater nucleation density, crystals grown under the partially compressed film were more uniform in size. This suggested that once the crystal nuclei formed, subsequent crystal growth would occur on these nuclei at the expense of fresh nucleation. On uncompressed films, nucleation was slow and led to both oriented vaterite and nonoriented calcite crystallization. This also implied the existence of condensed film islands, probably induced by the calcium ion binding strongly to the monolayer. Hence, although nucleation beneath films at lower surface pressures has been found to occur, it has always been at a reduced rate compared to nucleation at high surface pressures. Consequently, the mechanism of nucleation at lower surface pressures has always been attributed to nucleation beneath isolated clusters of condensed film material.

It has recently been shown,[21−24] however, that films at lower surface pressure may also possess a degree of order, even in the absence of film island formation. The application of techniques such as grazing incidence X-ray diffraction[25,26] and fluorescence microscopy[27,28] for determining the structure and packing of monolayers has been able to reveal such ordering. This has led some authors[23,24] to emphasize the apparently liquid−crystalline nature of these films.

In this study we investigate whether heterogeneous and epitaxial nucleation may occur *preferentially* upon such partially compressed or uncompressed films, i.e., *at a significantly greater rate than beneath the fully compressed films*. The decrease in order of these more expanded films, as compared with their fully compressed counterparts, may be compensated by their greater dynamical freedom and compressibility. Thus, a larger degree of lattice mismatch between the film and nucleating species may be accommodated. This idea is corroborated by a recent paper by Ahn *et al.*[29] on the dynamics of template-directed calcite crystallization under monolayer films. Using FTIR they were able to show that monolayers at medium surface pressures (10 mNm^{-1}) were actually able to reorganize themselves to optimize the geometrical and stereochemical fit between themselves and the growing crystal face. The optimized films had lattice parameters greater than those of the close-packed films, clearly indicating that a close-packed monolayer film, whether in the form of a coherent film or discrete islands, is *not* the only entity upon which nucleation beneath monolayer films can occur.

The following four film materials were used in this study: L-alanine octadecyl ester hydrochloride (L-ala film), L-aspartic acid tetradecyl diester hydrochloride (L-asp film), L-tyrosine *O*-octadecylcarbamoyl hydrochloride (L-tyr film), and its methyl ester, L-tyrosine *O*-octadecylcarbamoyl methyl ester hydrochloride (L-tyr-me film). These film materials afforded the best opportunity of observing nucleation of the amino acids beneath them, without their film headgroups completely matching the amino acids and thus biasing the nucleation toward crystallization of the face for which the film acted as a template. The amino acids, aspartic acid and asparagine, were chosen because they had suitable solubilities. The structures of the amino acids and film molecules used are shown schematically in Figure 1.

Experimental Section

Materials. Film compounds were synthesized from the purest available starting materials: L-alanine octadecyl ester hydrochloride was synthesized following the procedure of Penney *et al.*[30] and had a melting point of 112−114 °C; L-aspartic acid tetradecyl ester hydrochloride was synthesized following the procedure of Koch[31] and had a melting point of 109−111 °C; L-tyrosine *O*-octadecylcarbamoyl hydrochloride and its methyl ester were synthesized following the procedure of Marr-Leisy *et al.*[32] and had melting points of 197−198 °C and 163−164 °C, respectively. The NMR, infrared, and mass spectrometry data obtained from the film materials agreed with published data.[30−32]

The purity of the other materials used were as follows: L- and DL-aspartic acid (99%, BDH), D-, L-, and D,L-asparagine (99%, BDH), Milli-Q water (conductivity 0.05 μS/cm), chloroform (99.9%, Aldrich), and trifluoroacetic acid (99%, Aldrich).

Monolayer Experiments. The monolayer experiments were performed on a purpose-built computer-controlled Langmuir trough which enabled surface pressure, area, and time to be recorded. A Wilhelmy plate (consisting of a roughened platinum strip, 1 cm × 3 cm) attached to an Oertling NA114 microbalance was used to measure the surface pressure. The Langmuir trough was isolated in a rubber-mounted Perspex cabinet to reduce contamination and vibrations. The trough was sealed and saturated with water vapor to eliminate any effects of evaporation. The temperature in the trough was regulated to ±1 °C by a waterbath.

The trough was cleaned prior to each experiment with tissues soaked in chloroform followed by rinsing with Milli-Q water. Films were spread from approximately 1×10^{-3} M spreading solutions containing the following solvents: 96% chloroform and 4% trifluoroacetic acid for the L-ala, L-asp, and L-tyr-me films and for the L-tyr film, 86% chloroform, 10% methanol, and 4% trifluoroacetic acid. The Π-*A* isotherms were typically run in 3−5 min at a temperature of 20 ± 1 °C and to an accuracy of ±1 mNm^{-1} and ±1 $Å^2$.

Nucleation Experiments. Preparation of Supersaturated Solutions. The required amount of amino acid subphase material, determined from published solubility data,[33] was dissolved in 250 cm^3 of Milli-Q water by heating. This solution was filtered through 0.22 μm filters to remove any dust particles and was then maintained at a temperature at least 10 °C above its saturation temperature for a further hour. In the subsequent nucleation experiment, 210 cm^3 of the cooled solution was used while the remaining 40 cm^3 solution was left uncovered and acted as a control.

Control Experiments. Preliminary experiments were undertaken to determine the supersaturation limit for indiscriminate heterogeneous

(17) Majewski, J.; Popovitz-Biro, R.; Bouwman, W. G.; Kjaer, K.; Als-Nielson, J.; Lahav, M.; Leiserowitz, L. *Chem. Eur. J.* **1995**, *1*, 304−311.
(18) Grayer Wolf, S.; Leiserowitz, L.; Lahav, M.; Deutsch, M.; Kjaer, K.; Als-Nielson, J. *Nature* **1987**, *328*, 63−66.
(19) Barton, S. W.; Thomas, B. N.; Flom, E. B.; Rice, S. A.; Lin, B.; Peng, J. B.; Ketterson, J. B.; Dutta, P. *J. Chem. Phys.* **1988**, *89*, 2257−2270.
(20) Bloch, J. M.; Yun, W. B.; Yang, X.; Ramanathan, M.; Montano, P. A.; Capasso, C. *Phys. Rev. Lett* **1988**, *61*, 2941−2944.
(21) Kjaer, K.; Als-Nielson, J.; Helm, C. A.; Tippman-Krayer, P.; Möhwald, H. *J. Phys. Chem.* **1989**, *93*, 3200−3206.
(22) Lin, B.; Shih, M. C.; Bohanon, T. M.; Ice, G. E.; Dutta, P. *Phys. Rev. Lett.* **1990**, *65*, 191−194.
(23) Kenn, R. M.; Böhm, C.; Bibo, A. M.; Peterson, I. R.; Möhwald, H.; Als-Nielson, J.; Kjaer, K. *J. Phys. Chem.* **1991**, *95*, 2092−2097.
(24) Knobler, C. M. *J. Phys.: Condens. Matter*. **1991**, *3*, S17−S22.
(25) Kjaer, K.; Als-Nielson, J.; Helm, C. A.; Laxhuber, L. A.; Möhwald, H. *Phys. Rev. Lett.* **1987**, *58*, 2224−2227.
(26) Dutta, P.; Peng, J. B.; Lin, B.; Ketterson, J. B.; Prakash, M.; Georgopoulos, P.; Ehrlich, S. *Phys. Rev. Lett.* **1987**, *58*, 2228−2231.
(27) Lösche, M.; Rabe, J.; Fischer, A.; Rucha, B. U.; Knoll, W.; Möhwald, H. *Thin Solid Films* **1984**, *117*, 269−280.
(28) McConnell, H. M.; Tamm, L. K.; Weiss, R. M. *Proc. Natl. Acad. Sci. U.S.A.* **1984**, *81*, 3249−3253.
(29) Ahn, D. J.; Berman, A.; Charych, D. *J. Phys. Chem.* **1996**, *100*, 12455−12461.
(30) Penney, C. L.; Shah, P.; Landi, S. *J. Org. Chem.* **1985**, *50*, 1457−1459.
(31) Koch, H. *Doctoral Dissertation*; Johannes Gutenberg University: Mainz, Germany, 1983.
(32) Marr-Leisy, D.; Neumann, R.; Ringsdorf, H. *Colloid Polym. Sci.* **1985**, *263*, 791−798.
(33) Fasman, G. D. *Handbook of Biochemistry and Molecular Biology*, 3rd ed.; Chemical Rubber Co.: Cleveland, 1976; Vol. 1, p 115.

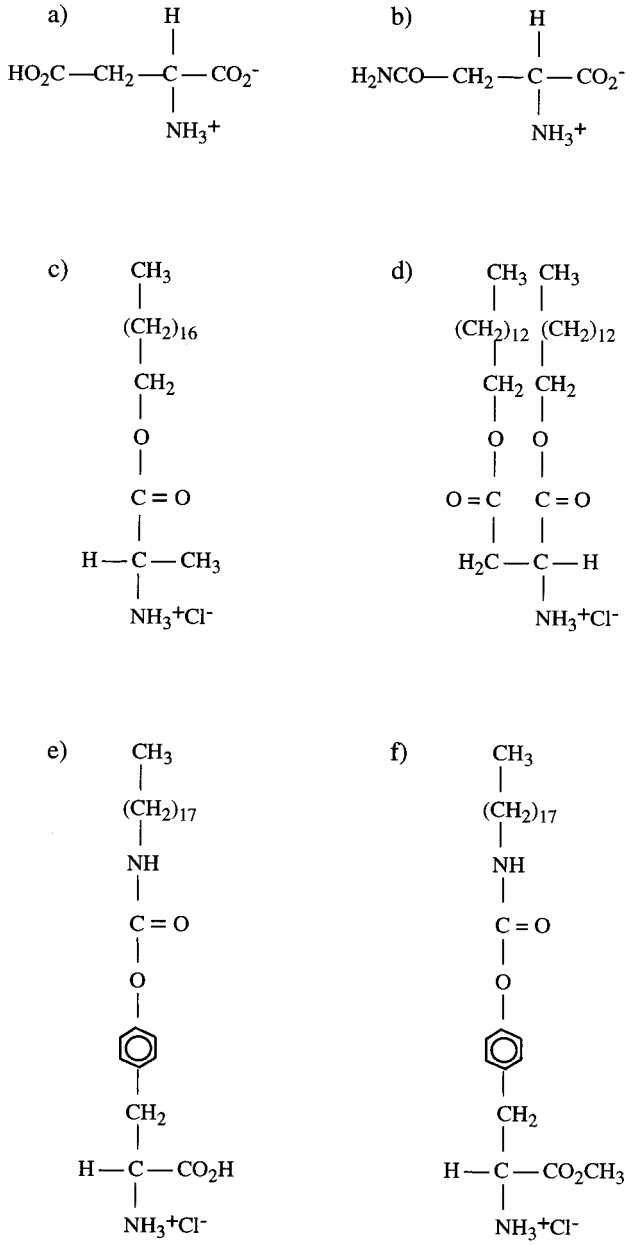

Figure 1. Schematic diagram of materials used in this study: (a) aspartic acid, (b) asparagine, (c) L-alanine octadecyl ester hydrochloride (L-ala film), (d) L-aspartic acid tetradecyl ester hydrochloride (L-asp film), (e) L-tyrosine *O*-octadecylcarbamoyl hydrochloride (L-tyr film), and (f) L-tyrosine *O*-octadecylcarbamoyl methyl ester hydrochloride (L-tyr-me film).

nucleation of the amino acids by dust particles, etc. The supersaturation limit for indiscriminate heterogeneous nucleation was defined as the lowest supersaturation at which a filtered, uncovered solution produced crystals in 24 h at ambient temperature. All the monolayer nucleation experiments were conducted at supersaturations below this value to ensure that any surface crystals observed did indeed nucleate beneath the film and not on any other foreign body.

Monolayer Nucleation Experiments. The monolayer nucleation experiments were performed using each different film material at ever decreasing supersaturations and at different initial film surface pressures. The temperature throughout the nucleation experiments was kept at 20 ± 2 °C. Glass slides were placed on the bottom of the PTFE trough to prevent nucleation occurring on scratches present there.

A typical monolayer nucleation experiment was performed using the following procedure. The film material was spread upon the supersaturated solution and approximately 3 min allowed for the spreading solvent to evaporate. The film was then compressed to the required surface pressure. The system was left undisturbed for 20 h, during which time the surface pressure was found to decrease.[34] For the first 3 h, the subphase surface was checked regularly, every 1/4 to 1/2 h, to ensure that no crystals were visible. This was important since any nuclei observed in this time would have either nucleated on dust particles or preexisted in the supersaturated solution, as insufficient time had elapsed for crystals nucleating beneath the monolayer film to grow to visible proportions. None of the experiments failed this test. Thereafter, the surface was checked at times of around 5, 7, and 20 h.

Analysis. At the end of each experiment, the surface crystals were carefully removed without disturbing their surface orientation using strips of pliable metal grid (grid size 0.5 mm). Typically, 60−80% of the surface crystals could be removed for surface analysis with their surface orientation preserved, although this value fell to approximately 50% at low supersaturations, where the crystals were smaller. All the crystals collected were dried with filter paper and viewed under an optical microscope. The crystals that exhibited clearly defined crystal faces were analyzed by single-crystal X-ray diffraction to determine the crystal face that grew beneath the film. With increasing experience, this face could be determined by inspection. The remaining crystals were glued onto the metal grids to preserve their surface orientation and were examined by scanning electron microscopy (SEM).

Results

Monolayer Experiments. Π-*A* Curves. Π-*A* curves of the films over aqueous subphases were in good agreement with the data reported in the literature.[31,32,35] Over saturated DL-aspartic acid and D,L-asparagine monohydrate solutions, the films became more expanded up to surface pressures of approximately 20−25 mNm^{-1}; this expansion effect was more marked for the L-tyrosine films. Above approximately 20−25 mNm^{-1}, the films became condensed and attained the same limiting areas per molecule as found for the films over aqueous solutions. This behavior was attributed to the adsorption of amino acid zwitterions *between* the film molecules up to surface pressures of approximately 20−25 mNm^{-1}.[36] Similar expansion effects in Π-*A* curves have also been observed in other systems where solute-film interactions were appreciable.[1,4,37−39]

Monolayer Experiments. Heterogeneous Nucleation Limit. Initial experiments upon nucleating L-aspartic acid beneath the films found that none of the films were particularly effective at promoting nucleation of this amino acid. Consequently, further experiments concentrated upon nucleation within the DL-aspartic acid and asparagine monohydrate systems, for which nucleation was more evident. Furthermore, owing to the small quantity of L-tyr film available, most of the monolayer nucleation experiments were conducted using the L-tyr-me film. The L-tyr experiments that were performed, however, all gave similar results to those of the L-tyr-me film.

Both the L-aspartic acid and L-alanine films were ineffective at promoting aspartic acid and asparagine monohydrate nucleation at supersaturations below that at which indiscriminate heterogeneous nucleation could occur. In contrast, the L-tyrosine films promoted nucleation down to supersaturations as low as $90 \pm 7\%$ and $40 \pm 5\%$ for DL-aspartic acid and D- and L-asparagine monohydrate, respectively.

DL-Aspartic Acid System. Effect of Surface Pressure. Table 1 shows the effect of surface pressure on DL-aspartic acid nucleation at supersaturations of 90%, 100%, 150%, and 200% under the L-tyr and L-tyr-me films. Nucleation was optimum under films at low to medium surface pressures. In contrast, nucleation on the surface between the barriers was significantly

(34) Gaines, G. I. *Insoluble Monolayers at Liquid−Gas Interfaces*; Interscience: New York, 1966; pp 151−155.
(35) Fukuda, K.; Shibasaki, Y.; Nakahara, H. *Macromol. Sci. Chem.* **1981**, *A15* (5), 999−1014.
(36) Cooper, S. J.; Sessions, R. B., Lubetkin, S. D. *Langmuir* **1997**, *13*, 7165−7172.

Table 1. Nucleation Rate of DL-Aspartic Acid beneath the L-Tyrosine Films as a Function of Supersaturation and Surface Pressure

film	supersaturation (%)	surface pressure range (mNm^{-1})	no. of surface crystals: inside barriers	no. of surface crystals: outside barriers
L-tyr-me	200	5 → 0	83	0
L-tyr-me	200	6 → 1	66	0
L-tyr-me	200	10 → 0	30	0
L-tyr-me	200	16 → 4	40	0
L-tyr-me	200	19 → 2	45	0
L-tyr-me	200	26→ 11	57	10
L-tyr-me	200	31 → 3	9[a]	20[a]
L-tyr-me	150	5 → 1	24	0
L-tyr-me	150	7 → 0	25	0
L-tyr-me	150	23 → 3	57	0
L-tyr	150	25 → 5	32	0
L-tyr-me	150	30 → 3	7[a]	7[a]
L-tyr-me	100	5 → 0	21	0
L-tyr-me	100	5 → 0	15	0
L-tyr-me	100	6 → 4	15	0
L-tyr-me	100	10 → 0	11	0
L-tyr-me	100	16 → 3	21	0
L-tyr-me	100	21 → 16	5	0
L-tyr	100	20 → 10	2	0
L-tyr-me	100	22 → 8	15	0
L-tyr-me	100	24 → 13	4	0
L-tyr-me	100	31 → 0	15[b]	6
L-tyr	100	35 → 5	1[a]	5[a]
L-tyr-me	100	57 → 26	5[a]	9[a]
L-tyr-me	90	19 → 5	7	0
L-tyr	90	15 → 3	4	0

[a] Nucleation beneath films compressed above ≈30 mNm^{-1} was significantly reduced, and more crystals tended to nucleate outside the barriers than within. The nucleation outside the barriers occurred on film material at low surface pressure that had dissolved from between the barriers and reemerged outside them. Even once the initial film surface pressure had decreased between the barriers due to this film dissolution, the nucleation rate was still low, since by then the supersaturation level had been reduced by nucleation on scratches in the PTFE trough. [b] The relatively high nucleation rate indicated here occurred many hours after the initial film compression, when the film was at far lower surface pressures. Nucleation could occur at this late stage, since nucleation did not occur on the PTFE trough at this supersaturation level.

reduced for films compressed to high surface pressures (above approximately 30 mNm^{-1}), while nucleation outside the barriers began to occur. The reduction in the nucleation rate in films compressed above 30 mNm^{-1} may be clearly seen in the entries marked by a superscript italic a in Table 1. Indeed, the number of crystals nucleating outside the barriers is typically greater than those nucleating within the barriers in these marked entries. The nucleation outside the barriers was found to arise due to dissolution of film molecules from between the barriers (evident from the rapid surface pressure drop following compression to high surface pressures) and their subsequent reemergence at the surface outside the barriers. The reemergence of film molecules outside the barriers caused the surface pressure there to rise to typically around 3 mNm^{-1}.

The lack of crystals nucleating between the barriers at high surface pressures, under the coherent, close-packed film, is evident from Figure 2, which shows the variation of the nucleation rate with surface pressure for the 100% supersaturated DL-aspartic acid and L-tyr-me film system. Since the coherent close-packed film was *not* an efficient nucleation promoter for DL-aspartic acid, it is *extremely unlikely* that the nucleation at lower surface pressures occurred beneath close-packed film islands, since the close-packed film itself did not induce nucleation.

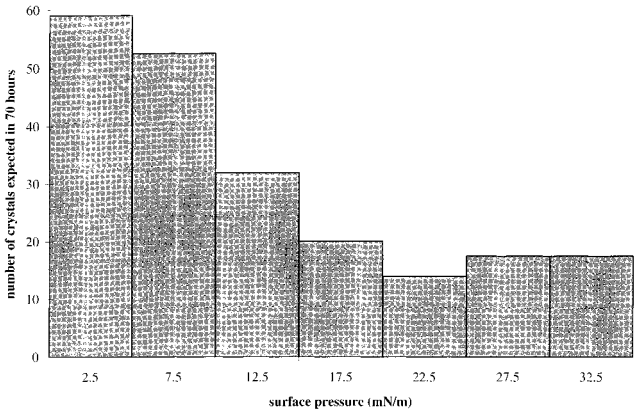

Figure 2. The histogram shows the variation in nucleation rate with surface pressure for the set of the 10 monolayer nucleation experiments on the 100% supersaturated DL-aspartic acid system using the L-tyr-me film shown in Table 1. The histogram was constructed by making the assumption that the nucleation rate does not vary during each nucleation experiment, so that the number of crystals nucleating in any surface pressure range is proportional to the time spent in that range. This assumption will *overestimate* the nucleation rate at the nonoptimal surface pressures. Hence the real variation in nucleation rate with surface pressure will fall off with increasing surface pressure even more rapidly than the histogram shows.

Crystal Morphology. The crystal faces that nucleated beneath the films exhibited numerous, often macroscopically visible, surface structure effects (see Figure 3). The large number of surface irregularities observed is typical of epitaxial nucleation.[40] In contrast, all other faces appeared flat and smooth.

Faces attached to the film were often enlarged compared with the corresponding faces of crystals grown from aqueous solution. This was expected from a diffusion limited growth mechanism, since this upper face is not in direct contact with the solution. All other faces present in the crystals were those commonly seen in aqueous solution, although the large size of faces attached to the films would sometimes mask the formation of the adjacent crystal faces.

Single crystal X-ray diffraction studies identified three types of crystal faces which commonly grew beneath the film: namely the {110}, {$\bar{1}$11}, and {$\bar{2}$02} faces, while on one occasion, the {$\bar{1}$12} face was also observed. The actual face that grew beneath the films was found to depend upon the surface pressure range in which the nucleation occurred. In particular, in the pressure range $\Pi \approx 7-25$ mNm^{-1} predominantly {$\bar{1}$11} nucleation occurred beneath the films, with a smaller proportion of {$\bar{2}$02} crystals also observed. Low surface pressures (<7 mNm^{-1}) produced significant nucleation of both the {$\bar{1}$11} and {110} faces, with a single case of {$\bar{1}$12} growth also observed. The ratio of different faces that grew beneath the films is shown in Table 2 for all the single crystals collected from under the films. The ratio values were calculated to the nearest half integer. In all the experiments, there was no discernible difference between DL-aspartic acid nucleation beneath the L-tyr film and its methyl ester, L-tyr-me.

Asparagine Monohydrate System. Effect of Surface Pressure. The effect of surface pressure on the nucleation of

(37) Arsentiev, V. A.; Leja, J. In *Colloid and Interface Scienc*; Kerker, M., Ed.; Academic Press: New York, 1976; vol. 5, pp 251−270.
(38) Chi, L. F.; Johnston, R. R.; Ringsdorf, H. *Langmuir* **1991**, *7*, 2323−2329.
(39) Ikeura, Y.; Kurihara, K.; Kunitake, T. *J. Am. Chem. Soc.* **1991**, *113*, 7342−7350.
(40) Stowell, M. J. In *Epitaxial Growth*; Matthews, J. W., Ed.; Academic Press: New York, 1975; Part B, p 437.

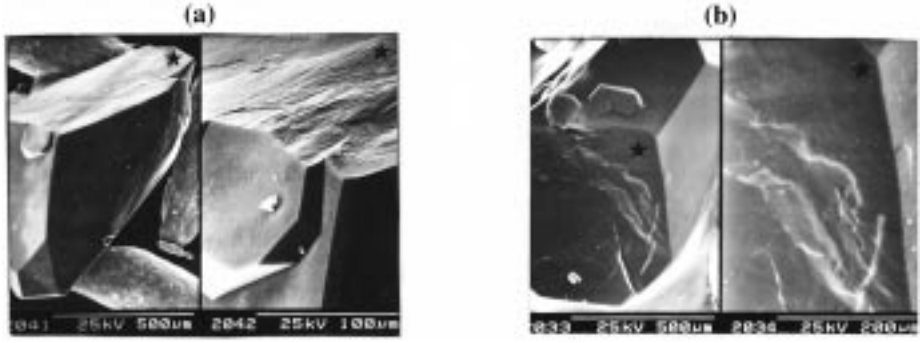

Figure 3. SEM micrographs of DL-aspartic acid crystals grown under the L-tyrosine films. The crystal face marked by an asterisk in the micrographs nucleated beneath the films. Note the high density of surface irregularities on this face, while all other faces are smooth. This is emphasized on the higher magnification pictures of this face on the right-hand side of each micrograph: (a) {110} growth and (b) $\{\bar{1}11\}$ growth.

Table 2. Ratio of Faces Found Nucleating beneath the Films in the DL-Aspartic Acid Experiments

film	supersaturation (%)	surface pressure range (mNm^{-1})	adsorbed DL-asp area per molecule ($Å^2$)	no. of surface crystals	ratio of faces nucleating beneath film $\{110\}:\{\bar{1}11\}:\{\bar{2}02\}:\{\bar{1}12\}$
L-tyr-me	200	5 → 0	≈ 65 → 100	83	4:2:1:0
L-tyr-me	200	6 → 1	≈ 60 → 97	66	2:2:1:0
L-tyr-me	150	5 → 1	≈ 65 → 93	24	8:3:1:0
L-tyr-me	150	7 → 0	≈ 56 → 100	25	2:1:0:0
L-tyr-me	100	5 → 0	≈ 65 → 100	21	1:1:0:0
L-tyr-me	100	5 → 0	≈ 65 → 100	15	5:3:2:1
L-tyr-me	100	6 → 4	≈ 60 → 76	15	1:1:0:0
L-tyr-me	200	10 → 0	≈ 46 → 100	30	1:3.5:0:0
L-tyr-me	200	16 → 4	≈ 39 → 66	40	4.5:2:1:0
L-tyr-me	200	19 → 2	≈ 37 → 83	45	4:7:1:0
L-tyr-me	100	10 → 0	≈ 46 → 100	11	1:2:1:0
L-tyr-me	100	16 → 3	≈ 39 → 82	21	1:1:0:0
L-tyr	100	20 → 10	≈ 34 → 45	2	0:1:1:0
L-tyr	90	15 → 3	≈ 39 → 74	4	1:1:1:0
L-tyr-me	90	19 → 5	≈ 35 → 66	7	1:1:1:0
L-tyr-me	200	26 → 11	≈ 30 → 45	57	0:4.5:1:0
L-tyr-me	150	23 → 3	≈ 32 → 80	57	1:7.5:4.5:0
L-tyr	150	25 → 5	≈ 32 → 59	32	1:3:2:0
L-tyr-me	100	21 → 16	≈ 34 → 39	5	0:1:1:0
L-tyr-me	100	22 → 8	≈ 32 → 55	15	0:3:1:0
L-tyr-me	100	24 → 13	≈ 31 → 44	4	0:1:1:0
L-tyr-me	200	31 → 3	≈ 28 → 83	9	1:1:0:0
L-tyr-me	150	30 → 3	≈ 28 → 81	7	2:1:0:0
L-tyr-me	100	31 → 0	≈ 28 → 100	15	1:1.5:1:0
L-tyr	100	35 → 5	≈ 28 → 59	1	1:0:0:0
L-tyr-me	100	57 → 26	≈ 26 → 30	5	2.5:1:0:0

asparagine monohydrate at supersaturations ranging from 30% to 92% is shown in Table 3. Nucleation beneath the films was optimum in the surface pressure range ≈5−20 mNm^{-1}. At higher surface pressures, the coherent films are again less effective at promoting asparagine nucleation. Similarly, at low surface pressures, asparagine nucleation is also less efficient. This lack of asparagine nucleation at low surface pressures ensures that, unlike in the DL-aspartic acid system, nucleation did not occur on the solution surface outside the barriers even if the films were compressed to high (>25 mNm^{-1}) surface pressures.

Crystal Morphology. The crystal faces attached to the L-tyrosine films were typically enlarged relative to their usual size in crystals grown from aqueous solution. Scanning electron micrographs of these faces (see Figure 4) revealed the presence not only of numerous surface irregularities but also "hopper" growth,[41,42] while all other faces appeared relatively smooth. Hopper growth on only one particular crystal face is frequently seen[42] in crystals growing on a melt surface, where growth upon the upper hopper face is limited since it is not in contact with the melt. Hence, the presence of "hoppers" on only one crystal face in the asparagine system confirms that this face did indeed nucleate beneath the film.

Single crystal X-ray diffraction studies identified two different crystal faces that grew predominantly beneath the L-tyrosine films: namely the {012} and {101} faces, while the {020} and {111} faces were seen on rare occasions. All other faces present in the crystals were those commonly seen in aqueous solution, although similarly to the DL-aspartic acid system, the large size of faces attached to the films would sometimes mask the formation of the adjacent crystal faces.

Discussion

In the monolayer experiments we have shown that nucleation (a) does not occur at the pure water surface outside the trough barriers; (b) is not caused by dust particles; and (c) is dramatically reduced under high surface pressure conditions where closed packed film is present. By contrast, nucleation occurs at a high rate beneath the film under conditions of low

(41) Pamplin, B. R. *Crystal Growth*; Pergamon: Oxford, 1975; pp 235, 239.

(42) Lefever, R. A.; Giess, E. A. *J. Am Ceram. Soc.* **1963**, *46*, 153−154.

Table 3. Nucleation Rate of Asparagine Monohydrate beneath the L-Tyrosine Films as a Function of Supersaturation and Surface Pressure

film	solute and its supersaturation level	surface pressure range (mNm^{-1})	no. of surface crystals inside barriers
L-tyr-me	92% D,L-asn	14 → 0	17
L-tyr	92% D,L-asn	15 → 0	20
L-tyr-me	87% L-asn	21 → 3	46
L-tyr	87% L-asn	22 → 3	54
L-tyr-me	87% D-asn	22 → 1	48
L-tyr	87% D-asn	22 → 7	51
L-tyr-me	53% D,L-asn	6 → 0	0
L-tyr-me	53% D,L-asn	9 → 0	5
L-tyr-me	53% D,L-asn	15 → 6	7
L-tyr	53% D,L-asn	14 → 0	7
L-tyr-me	53% D,L-asn	20 → 0	14
L-tyr-me	53% D,L-asn	26 → 0	4
L-tyr-me	53% L-asn	5 → 0	1
L-tyr-me	53% D-asn	5 → 0	0
L-tyr-me	53% L-asn	11 → 0	6
L-tyr-me	53% D-asn	12 → 0	4
L-tyr-me	53% L-asn	17 → 0	20
L-tyr-me	53% D-asn	14 → 0	11
L-tyr	53% L-asn	15 → 0	30
L-tyr	53% D-asn	15 → 0	12
L-tyr-me	53% L-asn	24 → 0	12
L-tyr-me	53% D-asn	20 → 13	4
L-tyr-me	45% L-asn	9 → 0	4
L-tyr-me	45% D-asn	11 → 0	3
L-tyr-me	40% L-asn	15 → 0	3
L-tyr-me	40% D-asn	14 → 0	3
L-tyr	40% L-asn	14 → 0	1
L-tyr	40% D-asn	14 → 0	4
L-tyr-me	30% D,L-asn	16 → 0	3
L-tyr	30% D,L-asn	17 → 0	2

to medium surface pressure. Thus, nucleation is occurring *preferentially* at low to medium surface pressures and not at high surface pressures, under the close−packed film, as previously observed.[3−5,7,8,13,14] This is a new finding, and as such we must look at the detailed mechanism of why the nucleation is biased toward these lower surface pressures. We must emphasize that the nucleation occurring at lower surface pressures is *highly unlikely* to be occurring under clusters of close-packed film; the close-packed film itself has been shown to be ineffective at promoting nucleation since the nucleation rate is greatly reduced at high surface pressures. Thus, although we cannot rule out the formation of close-packed film islands, we are of the firm opinion that they cannot be the main nucleators. Also, diffraction studies[18] on a similar α-amino acid monolayer have shown that close-packed film is only present above ≈15 mNm^{-1}; thus the surface pressure at which close-packed film material first appears correlates with the surface pressure at which we first observe a drop in nucleation rate. This is consistent with the close-packed film being a poor nucleator. Furthermore, both the Π-*A* expansion behavior of the films over the amino acid solutions and the adsorption modeling data[36] indicate that the amino acid zwitterions adsorb between the film molecules at low to medium surface pressures. This mitigates against close-packed film islands being present under these conditions.

The results strongly suggest that a new mechanism for nucleation beneath monolayer films is operating, whereby a property inherent in the lower surface pressure films is exploited, namely their increased compressibility. Such increased compressibility allows greater mismatches between the film and crystal face to be accommodated and so enables the nucleation beneath the films to occur, even though the film headgroups are not an exact match to the nucleating amino acids. The importance of the compressibility of the substrate has, of course, already been highlighted in epitaxial growth theory.[43] Furthermore, the recent paper by Ahn *et al.*[29] actually shows that a monolayer film at medium surface pressures can reorganize itself so as to reduce the lattice mismatch between itself and the growing crystal face.

The increased compressibility of lower surface pressure films will not be sufficient to induce nucleation in any species which does not match the film headgroup, unless there is a strong interaction between the two. In the present systems, this is demonstrated by the far greater nucleating power of the two L-tyrosine films compared with the L-aspartic acid and L-alanine films. The L-tyrosine films possess the two functional groups, NH_3^+ and CO_2CH_3 or CO_2H, upon which the amino acid zwitterions may bind, whereas both the L-aspartic acid and L-alanine films have only the NH_3^+ headgroup upon which amino acid binding may occur (see Figure 5). Therefore adsorption of the amine acid zwitterions between the film molecules will tend to be greater for the two L-tyrosine films; this agrees with the results of the adsorption calculations obtained from the Π-*A* curves of these systems.[36] In the present system, the "two point" interaction possible between the L-tyrosine films and amino acids will also help to predispose the resulting nucleation toward epitaxy, since the amino acid zwitterions may only adsorb between the L-tyrosine film molecules in a limited number of orientations if this favorable two point contact is to be maintained.

Correlation between the Modeled Structure of the Film and the Nucleating Crystal Face. In this study, both the amino acid nucleation rate and the crystal face nucleating beneath the film were dependent upon the surface pressure. This suggests that a degree of molecular recognition was occurring between the film and nucleating species. The film structures were modeled by placing the surfactant molecules at an area per molecule consistent with that calculated from the Π-*A* curves.[36] By comparing the structure of the nucleating faces to those of the modeled films, it is possible to determine whether this molecular recognition represents both a geometrical and stereochemical match between the film and nucleating crystal face or simply a strong electrostatic attraction between the two.

DL-Aspartic Acid System. There was a correlation between both the geometry and modeled structure of the film and nucleating crystal face in this case. The area, A_i, occupied by a zwitterion on the surface of each of the nucleating faces, namely the $\{\bar{1}11\}$, $\{110\}$, $\{\bar{2}02\}$, and $\{\bar{1}12\}$ faces, is 46.6, 80.0, 93.2, and 72.3 $Å^2$, respectively. In Table 4, these areas, A_i, are compared with the areas, A_{fx},[44] occupied by the DL-aspartic acid zwitterions adsorbed between the films at the nucleating surface pressures. For each crystal face, A_i lies within, or just outside, the range of A_{fx} values, i.e., $A_i \approx A_{fx}$. For the nucleation of the $\{\bar{1}11\}$ crystal face at low surface pressures, $2A_i \approx A_{fx}$, i.e., $\{\bar{2}22\}$ nucleation actually occurs. The crystal faces $\{\bar{1}11\}$, $\{110\}$, and $\{\bar{2}02\}$ each contain planes that are structurally similar to the film surface at that area. Hence, this suggests that both geometric and stereochemical recognition occurs between the film and nucleating crystal face. This is highlighted in Figure 6, which depicts suggested models for nucleation of these crystal faces under the film.

In the rarer case of $\{\bar{1}12\}$ nucleation, a regular array of film molecules (plus adsorbed amino acid zwitterions) is less likely

(43) Frank, F. C.; Van der Merwe, J. H. *Proc. R. Soc. London* **1949**, *A198*, 205−214, 215−220.

(44) The values of A_{fx} were determined by modeling the adsorption between the monolayer films using the Gibbs and Langmuir adsorption isotherms. The details of this approach may be found in ref 36.

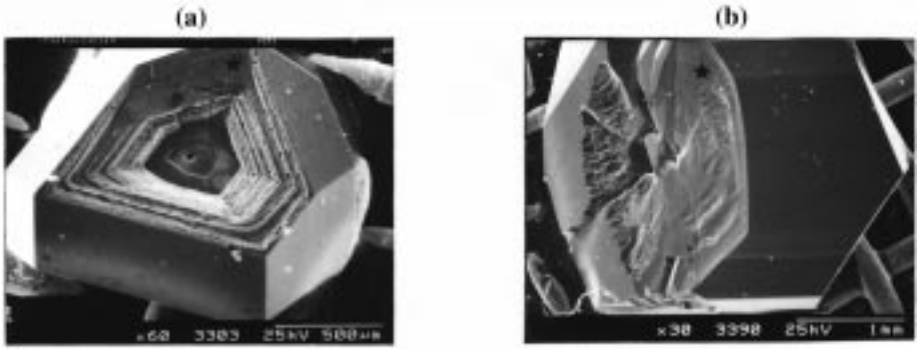

Figure 4. SEM micrographs of asparagine monohydrate crystals grown under the L-tyrosine films. The crystal face marked by an asterisk nucleated beneath the film. This face shows hopper growth in (a) and surface irregularities in (b) while all other faces are smooth. (a) and (b) both show {101} growth.

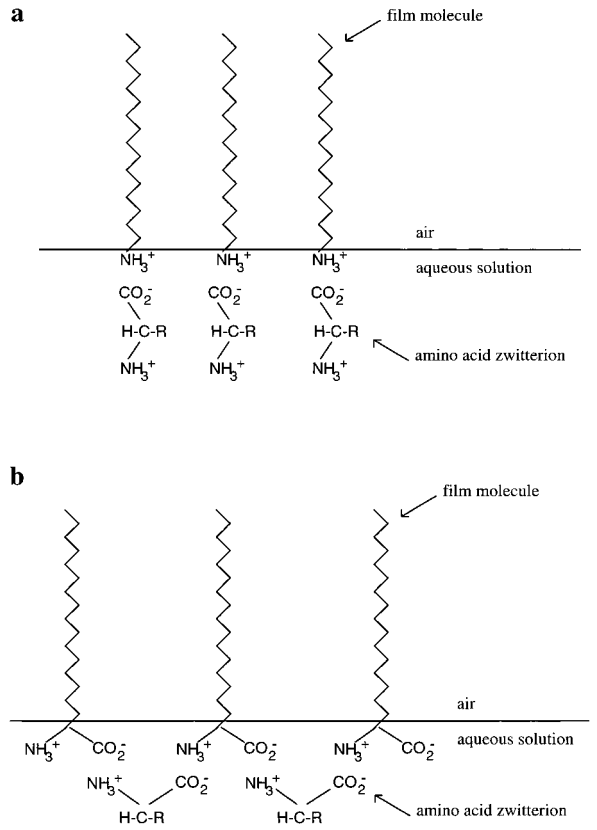

Figure 5. Schematic diagram of amino acid adsorption between the monolayer film molecules: (a) "single point" interaction between amino acids and L-ala and L-asp films and (b) "two point" interaction between amino acids and L-tyr and L-tyr-me films. R indicates the amino acid sidegroup.

to mimic this plane, since the face contains surface zwitterions with three distinct orientations. Consequently, no stereochemical recognition between the films and this face could occur. However, the $\{\bar{1}12\}$ plane does contain both positively, i.e., NH_3^+, and negatively, i.e., CO_2^-, charged surface groups. Thus, the single case of $\{\bar{1}12\}$ nucleation observed was induced by an electrostatic and geometric correlation between the film and crystal face.

The absence of nucleation at high surface pressures may be explained by the lack of a suitable (i.e., electrostatically compatible) crystal face with a small enough surface area per molecule. Modeling shows that the DL-aspartic acid zwitterions are larger than the film headgroups and so are unable to fit beneath the film when it is close-packed. Films at high surface pressures are less compressible, and any geometric mismatch between the film and nucleating crystal face is less easily accommodated. Hence nucleation will tend to be biased toward low to medium surface pressures in any system where there is not an exact match between the film headgroup and nucleating species, particularly when the nucleating species is larger than the film headgroup.

Therefore, in the DL-aspartic acid system, nucleation beneath the monolayer films appears to be governed by both a structural and geometric match between the film and nucleating crystal face.

Asparagine Monohydrate System. In each of the faces that nucleated beneath the films, namely the {012}, {101}, {020}, and {111} faces, the surface zwitterions have up to four different orientations. Hence, as with the $\{\bar{1}12\}$ DL-aspartic acid nucleation, stereochemical recognition could not occur. However, all these faces also contain positively and negatively charged groups. Thus, an electrostatic interaction between the film and these faces is a controlling factor in the nucleation. In addition, the nucleation rate is dependent upon the surface pressure; this suggests that geometric matching is also an important criterion.

Thus in the asparagine monohydrate system, nucleation beneath the films appears to be governed by both an electrostatic and geometric match between the films and nucleating faces.

L-Aspartic Acid System. We may also consider why the films were not efficient nucleators of L-aspartic acid. Nucleation of this amino acid would be facilitated if the low energy crystal face {100}, which dominates the aqueous crystal habit, could be nucleated. The structure of the stable[45] (100) plane contains only surface CO_2H groups and is therefore electrostatically incompatible with the L-tyrosine films. We would anticipate that this face could nucleate beneath the L-alanine and L-aspartic acid films which possess the NH_3^+ headgroup; however, the lack of a two point film-amino acid interaction prevents nucleation of this face occurring at the relatively low supersaturation levels investigated in this study.

Proposed New Mechanism for Nucleation beneath Monolayer Films. Previously, nucleation beneath monolayer films has been shown to occur preferentially under films at high surface pressures where the film is close-packed and ordered. In contrast, we have demonstrated preferential nucleation beneath films at low to medium surface pressures. It is *highly unlikely* that this nucleation is occurring under close-packed film islands, since the close−packed film itself was not an efficient nucleator. A property which is characteristic of the lower pressure films must be aiding the nucleation. In particular, we believe these novel results arise from the greater compressional

(45) Cooper, S. J.; Sessions, R. B. Manuscript in preparation.

Table 4. Comparison between A_i, the Area Occupied by Each Film Molecule on the Surface of the Crystal Face, the Range of A_{fx} Values at Which Nucleation of that Face Occurs, and the Maximum Area Mismatch Observed in This Nucleation

DL-aspartic acid crystal face	ca. range of nucleating surface pressures (mNm^{-1})	ca. range of nucleating areas per molecule, A_{fx} ($Å^2$)	area of molecule on nucleating face, A_i ($Å^2$)	max. area mismatch (%)
$\{\bar{1}11\}$	$\approx 0 \rightarrow 25$	$\approx 31 \rightarrow 100$	46.6, 93.2[a]	34
$\{\bar{2}02\}$	$\approx 7 \rightarrow 25$	$\approx 31 \rightarrow 56$	58.8	48
$\{\bar{1}12\}$ (rare)	$\approx 0 \rightarrow 7$	$\approx 56 \rightarrow 100$	72.3	38
{110}	$\approx 0 \rightarrow 7$	$\approx 56 \rightarrow 100$	80.0	30

[a] $\{\bar{2}22\}$ growth occurs.

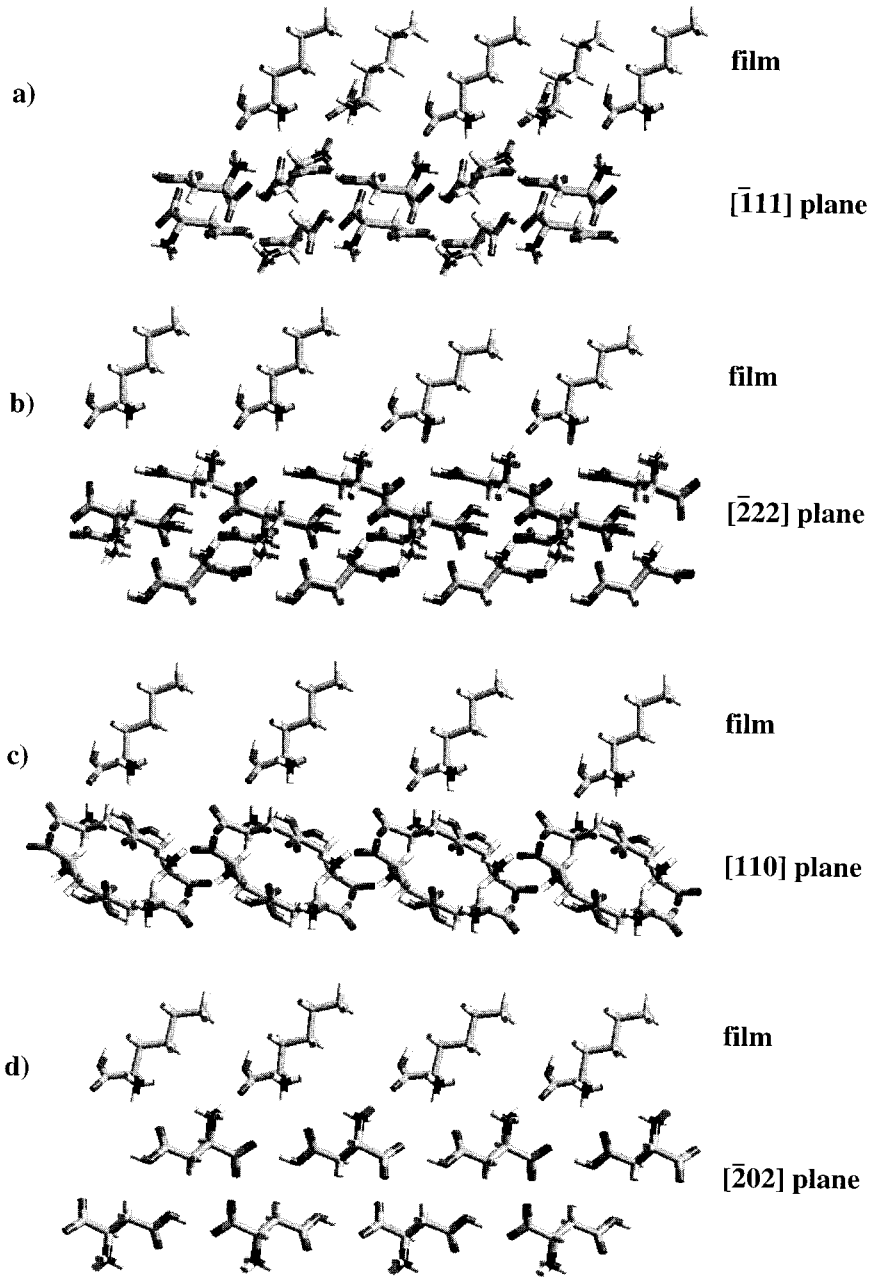

Figure 6. Suggested model for nucleation of crystal faces beneath the L-tyrosine films. Color code: carbon is shown in light gray, hydrogen in white, nitrogen in black, and oxygen in dark gray. Note only part of the L-tyrosine film has been shown for convenience. In each case the film mimics the face that nucleates beneath it. (a) $\{\bar{1}11\}$ growth beneath the films at surface pressures between ≈7 and 20 mNm^{-1}. (b) $\{\bar{2}22\}$ growth beneath the films at surface pressures <7 mNm^{-1}. (c) {110} growth beneath the films. (d) $\{\bar{2}02\}$ growth beneath the films.

freedom of films at lower surface pressures, which enables greater lattice mismatches between the film and nucleating crystal face to be accommodated.

We propose the nucleation is induced through the following processes: (1) the greater adsorption of the amino acids between the low to medium surface pressure film molecules, aided by the two point interaction between the two, and (2) the greater compressibility of the lower surface pressure films that allows the adsorbed amino acid layers to adopt conformations electrostatically and geometrically similar to layers within the

macroscopic crystal, thus inducing the corresponding faces to nucleate. This new mechanism for nucleation beneath monolayer films is likely to be important whenever the nucleating species and film headgroup are of a different nature, and particularly when the nucleating species is larger. Whereas nucleation under close-packed films typically results in the nucleation of one particular crystal face, nucleation at lower surface pressures will tend to be less specific, resulting in the nucleation of a number of low energy crystal faces.

Conclusion

We have shown that nucleation is undetectable on the pure water surface outside the trough barriers and occurs very slowly at high surface pressures beneath the fully compressed film. This demonstrates that neither the bare water surface nor fully packed films are good nucleators in this system. In contrast, the nucleation rate was high under low to medium surface pressures. Therefore nucleation beneath monolayer films is a phenomenon not only observed under films in a close-packed and ordered state. Indeed, nucleation beneath monolayer films is facilitated by having the film at lower surface pressures in systems where the film headgroup and nucleating species are not an exact match. We believe this behavior is explained by the "liquid−crystalline" type behavior of monolayer films at lower surface pressures; the films are more compressible and thus allow a greater geometric mismatch to be tolerated between the film and nucleating face, yet the films possess sufficient order to induce nucleation in any supersaturated species adsorbed strongly between them. This is the first time that nucleation beneath monolayer films has been shown to occur *preferentially* beneath films at low to medium surface pressures.

Acknowledgment. We would like to thank Dr. E. Bardishi for synthesizing most of the film materials. Dr. S. J. Cooper would like to thank SERC for financial support.

JA963799G